Contribution from the Laboratoire de Chimie des Métaux de Transition, Equipe de Recherche Associée au CNRS No. 608, Université P. et M. Curie, 75231 Paris, France, and the Laboratoire de Spectrochimie des Elêments de Transition, Equipe de Recherche Associée au CNRS No. 672, Université de Paris Sud, 91405 Orsay, France

Crystal Structure and Magnetic Properties of Tetrakis(cyclohexylamine)di-μ-hydroxo-dicopper(II) Perchlorate. The First Example of a Roof-Shaped Hydroxo-Bridged Copper(II) Dimer

M. F. CHARLOT,[1a] S. JEANNIN,[1b] Y. JEANNIN,*[1b] O. KAHN,*[1a] J. LUCRECE-ABAUL,[1b] and J. MARTIN-FRERE[1b]

Received November 27, 1978

The title compound $[Cu(C_6H_{11}NH_2)_2OH]_2(ClO_4)_2$ was synthesized and its crystal structure solved at room temperature from 6429 independent reflections. It crystallizes in the monoclinic system, space group $C2/c$. The lattice constants are $a = 27.77$ (1) Å, $b = 14.45$ (1) Å, $c = 17.68$ (1) Å, and $\beta = 91.7$ (1)° with $Z = 8$. Least-squares refinement of the structure led to a conventional weighted R factor of 0.069 excluding zeros. High thermal vibrations of perchlorate groups and cyclohexyl rings limited the refinement. The structure is made of roof-shaped binuclear units $[Cu(C_6H_{11}NH_2)_2OH]_2^{2+}$ with a dihedral angle of 147.5° and of essentially noncoordinated perchlorate anions. The temperature dependence of the magnetic susceptibility, studied in the range 10–300 K, shows an intramolecular antiferromagnetic coupling with a singlet–triplet separation of −256 cm^{-1}. According to Hatfield and Hodgson's correlation, the planar hydroxo-bridged Cu(II) dimer derived from the title compound by opening the dihedral angle up to 180° should exhibit a singlet–triplet separation of about −600 cm^{-1}. The influence of the bending on the magnetic properties was studied in the framework of a previously described orbital model.

Introduction

In the last few years, a large number of works were devoted to the synthesis of Cu(II) binuclear complexes, the determination of their crystal structures, and the investigation of their magnetic properties.[2-16] The main goal of most of these works was a better understanding of the phenomenon of exchange interaction. Important results were already obtained in this way. Among these results of particular interest is the one stated by Hatfield, Hodgson, and their co-workers.[6,7] They studied eight hydroxo-bridged Cu(II) dimers and established a linear correlation between the values of the J singlet–triplet energy gap and of the Cu–O–Cu bridging angle. A theoretical justification of this result was proposed by Hoffmann and co-workers.[16] Seven of the eight hydroxo-bridged Cu(II) dimers were planar or nearly planar. The last one contained a nonplanar Cu_2O_2 network with pentacoordinated copper(II) in a distorded square-pyramidal configuration and a dihedral angle between the two CuO_2 planes of 174°.[17] The value of the J parameter for this compound also supported the linear correlation between J and Cu–O–Cu. However, owing to the weak deviation from a planar structure it was difficult to assert from this result that this correlation was valid for roof-shaped hydroxo-bridged Cu(II) dimers whatever the dihedral angle may be. In other respects, the theoretical justification presented by Hoffmann as well as the purely qualitative approach of Hatfield and Hodgson concerned only Cu(II) dimers with a strictly planar Cu_2O_2 network. Bencini and Gatteschi, however, recently studied the effect of various distortions from an angular overlap approach.[18]

We have synthesized a new hydroxo-bridged Cu(II) dimer and studied its crystal structure. This complex is the first one which is roof-shaped with a dihedral angle of 147.5°. The investigation and the interpretation of its magnetic properties were therefore particularly interesting. Correlating crystal structure and magnetic behavior, we believe we bring a new and significant contribution to the understanding of the exchange interaction in Cu(II) dimers.

Experimental Section

Synthesis. A total of 5 cm^3 of a 10 M solution of cyclohexylamine in methanol was poured into 50 cm^3 of a 5×10^{-2} M solution of copper(II) perchlorate hexahydrate in ethanol. A slow evaporation of this solution under nitrogen current, at room temperature, led to blue crystals which were filtered out and dried under nitrogen.

Anal. Calcd for $CuC_{12}H_{27}N_2O_5Cl$: Cu, 16.81; C, 38.11; H, 7.14; N, 7.41; Cl, 9.38. Found: Cu, 16.7; C, 38.13; H, 6.96; N, 7.30; Cl, 9.37.

Crystal Structure and Refinement. The compound is slightly air sensitive leading to a white cyclohexylamine carbonate powder owing to the carbon dioxide action. The crystal selected for X-ray analysis was roughly parallelepiped shaped with $0.62 \times 0.28 \times 0.04$ mm dimensions. It was screened with varnish and set up on the goniometric head along its 001 axis. Preliminary Laue and precession photographs led to a monoclinic unit cell. Lattice constants were obtained from precession photographs, by using a Siemens coincidence rule, and from diffractometer settings. Two space groups were possible from systematic absences: $C2/c$ and Cc. Statistical tests on normalized structure factors,[19a] Rogers' method[19b] and a nonlinear optical method led to $C2/c$: $a = 27.77$ (1) Å, $b = 14.45$ (1) Å, $c = 17.68$ (1) Å, $\beta = 91.7$ (1)°, for $Z = 8$ ρ(measd) (flotation in a trichloroethane–o-dichlorobenzene mixture) = 1.42 ± 0.02 g cm^{-3} and ρ(calcd) = 1.43 g cm^{-3}, $V = 7094$ Å^3.

Intensity data were collected on an automatic Enraf Nonius CAD 3 diffractometer: radiation was Cu Kα filtered with nickel, crystal focus distance was 235 mm, crystal–counter distance was 87 mm, scintillation counter was connected to a height pulse analyzer set on Cu Kα energy so that 90% of the intensity was counted, filters were used to decrease high countings and to avoid counting losses, several counting cycles were repeated for low-intensity reflections, so that accumulated integrated intensity reaches about 3000 impulses/s, scan type was $\theta/2\theta$ (1/6° s^{-1}), scan length was 1.20° symmetrical scan at zero Bragg angle, corrected for $K\alpha_1$–$K\alpha_2$ dispersion, background measurements were in fixed position before and after every scan, during $t' = t/2$, where t is the scan duration, two standard reflections, 080 and $\bar{1}2,0,0$, were measured every 41 reflections, 6429 independent reflections were collected at 21 °C up to $\theta_{Bragg} = 66°$. Intensities were corrected from Lorentz polarization. Intensity variations of standard reflections were linear with a maximum 25% decrease; intensities were corrected from these variations. The absorption coefficient was equal to 33.5 cm^{-1}; corrections were calculated and intensities were then corrected. Transmission factors varied from 0.36 to 0.87. For every observed structure factor F_o, a standard deviation σ was computed: $\sigma = F_o\Delta C/2C$, where C is the integrated intensity and ΔC the error on it; 2784 reflections for which integrated intensities were lower than 3σ were excluded. Atomic form factors were taken from Cromer and Waber[20] for all the atoms except for hydrogen atoms for which values of Stewart, Davidson, and Simpson[21] were applied. The copper and chlorine atoms were corrected for real and imaginary parts of anomalous dispersion. Refinements were carried out by full-matrix least squares, minimizing the R_w factor

$$R_w = [\sum_i (w_i|F_o - kF_c|)^2 / \sum_i |w_i F_o|^2]^{0.5}$$

0020-1669/79/1318-1675$01.00/0

Table I. Atomic Coordinates ($\times 10^4$)[a]

atom	x	y	z	atom	x	y	z
Cu_1	8094.3 (4)	6820.8 (8)	1441.7 (6)	C_{62}	8988 (3)	4357 (7)	1130 (10)
Cu_2	7899.8 (4)	8224.7 (7)	274.9 (6)	$H_1(C_{62})$	8683	4062	939
O_2	7963 (2)	6872 (3)	347 (3)	$H_2(C_{62})$	9047	4115	1679
$H(O_2)$	8232	6622	47	C_{13}	8753 (3)	8439 (7)	−718 (6)
O_3	7744 (2)	7957 (3)	1300 (3)	$H(C_{13})$	8774	9116	−563
$H(O_3)$	7872	8458	1651	C_{23}	8949 (4)	8395 (9)	−1507 (7)
N_1	8173 (2)	6990 (5)	2563 (4)	$H_1(C_{23})$	8738	8787	−1870
$H_1(N_1)$	8072	6412	2816	$H_2(C_{23})$	8906	7721	−1704
$H_2(N_1)$	7946	7510	2712	C_{33}	9491 (6)	8658 (13)	−1487 (14)
N_2	8437 (3)	5605 (4)	1428 (5)	$H_1(C_{33})$	9515	9364	−1377
$H_1(N_2)$	8228	5197	1101	$H_2(C_{33})$	9623	8606	−2035
$H_2(N_2)$	8437	5381	1960				
N_3	8230 (2)	8244 (5)	−723 (3)	C_{43}	9782 (5)	8152 (15)	−909 (17)
$H_1(N_3)$	8064	8726	−1047	$H_1(C_{43})$	10119	8365	−946
$H_2(N_3)$	8183	7623	−963	$H_2(C_{43})$	9775	7472	−1129
N_4	7769 (3)	9590 (4)	346 (4)	C_{53}	9567 (5)	8195 (14)	−138 (13)
$H_1(N_4)$	7420	9645	484	$H_1(C_{53})$	9590	8852	61
$H_2(N_4)$	7803	9839	−180	$H_2(C_{53})$	9762	7788	228
C_1	8655 (3)	7248 (6)	2877 (5)	C_{63}	9024 (4)	7915 (9)	−135 (7)
$H(C_1)$	8877	6706	2788	$H_1(C_{63})$	8884	7986	388
C_2	8640 (4)	7411 (7)	3723 (6)	$H_2(C_{63})$	8996	7203	−249
$H_1(C_2)$	8551	6823	3991	C_{14}	8038 (4)	10234 (6)	826 (8)
$H_2(C_2)$	8401	7902	3841	$H(C_{14})$	7877	9941	1292
C_3	9149 (5)	7704 (11)	4012 (9)	C_{24}	8535 (5)	10108 (8)	959 (9)
$H_1(C_3)$	9394	7196	3975	$H_1(C_{24})$	8672	10209	429
$H_2(C_3)$	9153	7928	4557	$H_2(C_{24})$	8593	9481	1120
C_4	9344 (5)	8504 (11)	3595 (12)	C_{34}	8795 (5)	10781 (9)	1424 (9)
$H_1(C_4)$	9154	9069	3662	$H_1(C_{34})$	9145	10705	1359
$H_2(C_4)$	9696	8639	3752	$H_2(C_{34})$	8735	10548	1988
C_5	9343 (3)	8333 (9)	2765 (9)	C_{44}	8642 (7)	11728 (10)	1397 (9)
$H_1(C_5)$	9582	7795	2665	$H_1(C_{44})$	8751	12007	882
$H_2(C_5)$	9467	8883	2489	$H_2(C_{44})$	8792	12131	1799
C_6	8852 (3)	8052 (6)	2449 (6)	C_{54}	8158 (10)	11853 (10)	1332 (17)
$H_1(C_6)$	8626	8589	2487	$H_1(C_{54})$	8080	11641	1915
$H_2(C_6)$	8871	7876	1894	$H_2(C_{54})$	8095	12505	1321
C_{12}	8909 (3)	5397 (7)	1206 (9)	C_{64}	7852 (4)	11219 (6)	775 (7)
$H(C_{12})$	8783	5610	683	$H_1(C_{64})$	7495	11247	880
C_{22}	9330 (4)	5880 (9)	1376 (12)	$H_2(C_{64})$	7891	11451	238
$H_1(C_{22})$	9301	6034	1918	Cl_1	7724.7 (8)	9644 (1)	3295 (1)
$H_2(C_{22})$	9250	6532	1091	O_{11}	8191 (2)	9690 (5)	3672 (5)
C_{32}	9775 (5)	5597 (10)	1201 (14)	O_{12}	7728 (3)	9013 (6)	2696 (4)
$H_1(C_{32})$	10002	5859	1598	O_{13}	7385 (3)	9342 (5)	3842 (5)
$H_2(C_{32})$	9864	5914	696	O_{14}	7587 (2)	10553 (4)	3056 (4)
C_{42}	9859 (5)	4607 (10)	1128 (15)	Cl_2	6491 (1)	9580 (2)	1333 (2)
$H_1(C_{42})$	10168	4455	847	O_{21}	6086 (6)	9923 (13)	1432 (15)
$H_2(C_{42})$	9884	4286	1630	O_{22}	6827 (6)	10115 (7)	1719 (8)
C_{52}	9457 (8)	4146 (12)	710 (22)	O_{23}	6571 (9)	8708 (13)	1456 (24)
$H_1(C_{52})$	9376	4479	146	O_{24}	6570 (9)	9484 (25)	638 (10)
$H_2(C_{52})$	9457	3481	564				

[a] Standard deviations on the last significant figures are given in parentheses.

where w is $1/\sigma$ and k is the scale factor.

A three-dimensional Patterson map showed copper and chlorine atoms. Refinement of their coordinates led to $R = 0.35$. Successive Fourier syntheses and refinements dropped R to 0.147 with isotropic temperature factors and to 0.088 with anisotropic temperature factors. Introduction of 54 hydrogen atom coordinates led to $R = 0.081$. A total of 37 reflections for which differences of $|F_o - F|$ were higher than 15 were excluded from refinement. Final reliability factors are as follows: nonweighted R excluding zeros, 0.069; weighted R excluding zeros, 0.071; $F(000) = 1813$. The atomic parameters are shown in Table I and anisotropic thermal parameters in Table II. Main interatomic distances and bond angles are given in Table III. Two ORTEP[22] diagrams were computed with 20 and 50% probability thermal ellipsoids (Figures 1 and 2).

Magnetic Measurements. Magnetic measurements were carried out on two powder samples in the temperature range 10–312 K with a Faraday-type magnetometer, equipped with a continuous flow cryostat designed by Oxford Instruments. The temperature was given by a gold–iron/chromel thermocouple. A magnetic induction of about 9 kG was used. The independence of the susceptibility from the magnetic induction was checked at room temperature; this gives evidence of the absence of ferromagnetic impurities in the sample. Mercuritetrathiocyanatocobaltate(II) was used as a susceptibility standard. The absolute accuracy on temperature was estimated at ±0.1 K and the relative accuracy on the apparent increase of the weight of the sample when the magnetic field was applied was about 1%.

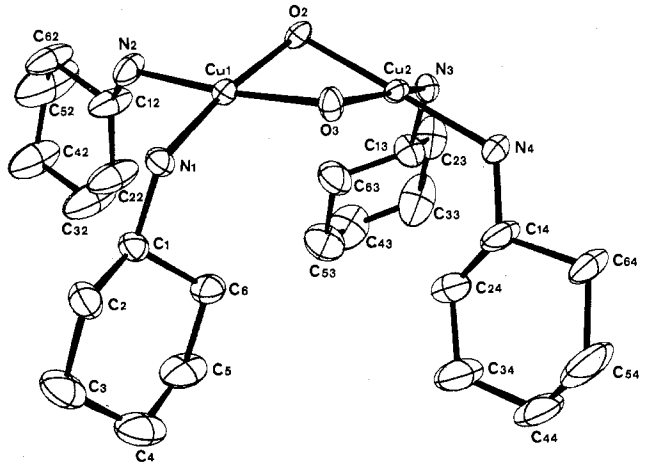

Figure 1. ORTEP drawing of complex dimeric cation, with 20% probability thermal ellipsoids.

Table II. Atomic Thermal Parameters[a]

atom	B_{11}	B_{22}	B_{33}	B_{12}	B_{13}	B_{23}
Cu_1	3.91 (5)	3.03 (4)	4.16 (5)	−0.04 (4)	−0.13 (4)	0.06 (4)
Cu_2	4.51 (5)	2.89 (4)	3.56 (5)	−0.44 (4)	−0.17 (4)	−0.35 (4)
O_2	5.4 (3)	2.5 (2)	4.5 (2)	−0.1 (2)	−0.9 (2)	−0.5 (2)
O_3	6.4 (3)	3.6 (2)	3.8 (2)	1.7 (2)	−0.9 (2)	−0.3 (2)
N_1	3.6 (3)	5.1 (4)	4.5 (3)	−0.4 (2)	−0.6 (2)	−0.8 (3)
N_2	5.1 (4)	3.0 (3)	10.7 (6)	0.5 (3)	0.7 (4)	0.6 (3)
N_3	4.9 (3)	4.5 (3)	3.8 (3)	0.2 (3)	0.2 (2)	0.8 (3)
N_4	6.8 (4)	3.2 (3)	5.8 (4)	−0.2 (3)	−0.9 (3)	0.0 (3)
C_1	4.8 (4)	4.4 (4)	5.3 (4)	0.8 (3)	−1.1 (3)	−0.5 (3)
C_2	8.5 (7)	5.8 (7)	6.2 (6)	1.5 (5)	−2.4 (5)	−0.3 (4)
C_3	7.4 (7)	9.7 (9)	10.5 (9)	3.0 (6)	−4.5 (7)	−2.3 (7)
C_4	6.2 (7)	9.8 (9)	14 (1)	0.6 (6)	−4.2 (7)	−3.8 (9)
C_5	3.1 (4)	8.3 (7)	15 (1)	−0.9 (4)	−0.5 (5)	−1.5 (8)
C_6	4.3 (4)	5.2 (5)	8.1 (6)	−0.8 (4)	−0.9 (4)	−0.0 (4)
C_{12}	2.8 (4)	4.6 (5)	19 (1)	0.4 (4)	0.4 (5)	−2.3 (6)
C_{22}	5.4 (6)	6.5 (6)	21 (2)	−1.0 (5)	2.7 (7)	−3.5 (8)
C_{32}	6.9 (8)	7.3 (8)	27 (2)	−1.0 (6)	2 (1)	−3 (1)
C_{42}	6.4 (7)	6.0 (7)	29 (2)	1.2 (6)	0.7 (9)	−2.7 (9)
C_{52}	11 (1)	6.4 (9)	46 (4)	2.7 (9)	4 (2)	−5 (1)
C_{62}	4.2 (5)	4.3 (5)	20 (1)	−0.2 (4)	1.6 (7)	−2.5 (6)
C_{13}	4.5 (4)	7.9 (6)	6.1 (5)	0.3 (4)	1.0 (4)	0.9 (4)
C_{23}	7.6 (6)	9.1 (8)	9.3 (8)	2.6 (6)	4.2 (6)	2.4 (6)
C_{33}	8.9 (9)	11 (1)	20 (2)	3.0 (8)	8 (1)	4 (1)
C_{43}	5.1 (7)	12 (1)	25 (2)	0.4 (8)	3 (1)	2 (1)
C_{53}	4.9 (6)	13 (1)	18 (2)	−0.7 (8)	−2.6 (8)	2 (1)
C_{63}	5.6 (5)	10.2 (8)	9.8 (8)	−0.6 (5)	−1.4 (5)	2.1 (6)
C_{14}	6.7 (6)	3.6 (4)	13.3 (9)	−0.3 (4)	−0.1 (6)	2.8 (5)
C_{24}	9.6 (8)	5.8 (6)	13 (1)	−1.1 (6)	−3.8 (8)	−1.9 (7)
C_{34}	9.4 (8)	7.4 (7)	14 (1)	−2.7 (6)	−0.6 (8)	−3.0 (7)
C_{44}	14 (1)	5.9 (7)	12 (1)	−5.4 (8)	−0.5 (9)	−0.9 (7)
C_{54}	17 (1)	4.4 (6)	30 (3)	1.0 (9)	−3 (2)	−6 (1)
C_{64}	8.9 (7)	3.3 (4)	10.7 (8)	−0.7 (4)	1.0 (6)	−1.7 (5)
Cl_1	5.1 (1)	4.1 (1)	5.5 (1)	1.1 (1)	−0.2 (1)	−1.4 (1)
O_{11}	6.5 (4)	5.8 (3)	10.8 (5)	1.2 (3)	−1.5 (3)	−2.3 (3)
O_{12}	11.8 (6)	8.3 (4)	7.0 (4)	3.8 (4)	−2.2 (4)	−4.5 (4)
O_{13}	8.9 (5)	7.8 (4)	8.4 (5)	1.5 (4)	1.9 (4)	1.3 (4)
O_{14}	6.7 (3)	4.5 (3)	7.3 (4)	0.7 (3)	0.6 (3)	0.6 (3)
Cl_2	5.8 (1)	7.6 (2)	10.1 (2)	−0.2 (1)	−0.0 (1)	−5.1 (1)
O_{21}	11.2 (9)	18 (1)	34 (2)	2.0 (8)	5 (1)	−7 (1)
O_{22}	20 (1)	8.4 (5)	16.8 (9)	−1.8 (6)	−7.2 (9)	−3.9 (6)
O_{23}	26 (2)	10 (1)	48 (4)	1 (1)	−5 (3)	
O_{24}	27 (2)	45 (4)	10.3 (9)	10 (2)	−2 (1)	

[a] The anisotropic thermal parameters have units of Å². They enter the expression for the structure factor in the form $\exp[-0.25\cdot(B_{11}h^2a^{*2} + B_{22}k^2b^{*2} + B_{33}l^2c^{*2} + 2B_{12}hka^*b^* + 2B_{23}klb^*c^* + 2B_{13}hla^*c^*)]$. Standard deviations on the last significant figures are given in parentheses.

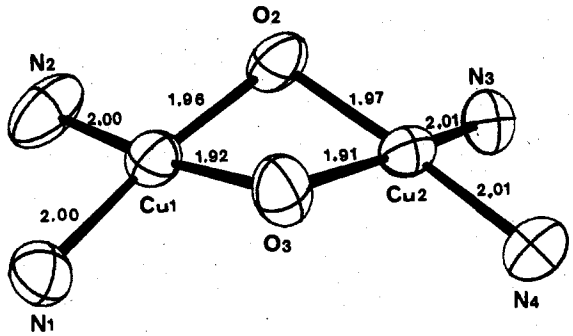

Figure 2. ORTEP drawing of the roof-shaped hydroxo-bridged copper(II), with 50% probability thermal ellipsoids and bond lengths.

The correction for diamagnetism was estimated at -404×10^{-6} cm³ mol⁻¹ from the atomic values of Pascal.[23]

Results and Discussion

Crystal Structure. Each asymmetric unit contains a complex dimeric cation (Figure 1) and two perchlorate ions. Both copper atoms of the complex cation are linked through a double hydroxo bridge, leading to a copper–copper distance of 2.93 ± 0.02 Å.

The surrounding of each copper atom is square planar; it consists of the two bridging hydroxo groups O_2 and O_3 and of two cyclohexylamine molecules coordinated through their nitrogen atom. Deviations of atoms from the mean planes

Table III. Main Interatomic Distances and Bond Angles[a]

Distances, Å			
Cu-Cu Distance			
Cu_1-Cu_2	2.934 (8)		
Cu Surrounding			
Cu_1-O_2	1.960 (5)	Cu_2-O_2	1.967 (5)
Cu_1-O_3	1.923 (5)	Cu_2-O_3	1.914 (6)
Cu_1-N_1	2.003 (7)	Cu_2-N_3	2.012 (7)
Cu_1-N_2	2.002 (7)	Cu_2-N_4	2.013 (7)
Angles, Deg			
Dihedral Angle			
$Cu_1O_2O_3$ and $Cu_2O_2O_3$[b]	147.5 (8)		
Cu Surrounding			
O_2-Cu_1-O_3	76.1 (2)	O_2-Cu_2-O_3	76.1 (2)
N_1-Cu_1-N_2	94.7 (3)	N_3-Cu_2-N_4	97.4 (3)
O_2-Cu_1-N_2	95.6 (3)	O_2-Cu_2-N_3	91.6 (2)
O_3-Cu_1-N_1	93.7 (3)	O_3-Cu_2-N_4	95.4 (3)
Bridging Angles			
Cu_1-O_2-Cu_2	96.6 (2)	Cu_1-O_3-Cu_2	99.7 (2)

[a] Standard deviations on the last significant figures are given in parentheses. [b] The dihedral angle between $Cu_1O_2O_3$ and $Cu_2O_2O_3$ planes.

Table IV. Mean Planes of the Copper Square-Planar Surrounding and Deviations of Atoms from These Planes

Cu_1 surrounding		Cu_2 surrounding	
atom	dev, Å	atom	dev, Å
Cu_1	−0.002	Cu_2	+0.06
O_2	−0.014	O_2	+0.13
O_3	+0.015	O_3	−0.14
N_1	−0.012	N_3	−0.13
N_2	+0.012	N_4	+0.08

$Cu_1O_2O_3N_1N_2$ and $Cu_2O_2O_3N_3N_4$ have been calculated (Table IV); they show that the Cu_2 surrounding slightly deviates from planarity. The bond lengths are shown in Table III and Figure 2. All Cu–N bonds are equal within experimental errors, but Cu–O bonds are slightly different as far as standard deviations are concerned: each hydroxo group is symmetrically bound, with O_3–Cu bonds shorter than O_2–Cu bonds. Also, it can be seen that the Cu_1–O_2–Cu_2 angle is equal to 96.6 ± 0.6° and Cu_1–O_3–Cu_2 angle is equal to 99.7 ± 0.6°; these values are similar to those found in other hydroxo-bridged copper dimers usually ranging from 95 to 105°.[6,7] However, the most interesting and unusual feature of this structure is the dihedral angle observed between the planes $Cu_1O_2O_3$ and $Cu_2O_2O_3$, which is equal to 147.5°; it is the first example of a roof-shaped bridge, with such a closed angle, so different from 180°. The dihedral angle between the two mean planes of the copper square-planar surroundings is not very different, equal to 144°.

Perchlorate ions are not coordinated to copper atoms. The shortest Cu–ClO_4 distance, observed between Cu_1 and the oxygen atom O_{14} of the first perchlorate, is equal to 2.8 Å, which might suggest only a very weak interaction with Cu_1, the surrounding of which would be a square pyramid with its apex occupied by O_{14}. The O_{14}–Cu_1 direction is not exactly perpendicular to the mean basal plane $O_2O_3N_1N_2$: the angle is equal to 71°. Angles around Cu_1 and involving O_{14} are O_{14}–Cu_1–N_1 = 79.8°, O_{14}–Cu_1–N_2 = 75.8°, O_{14}–Cu_1–O_2 = 103.3°, and O_{14}–Cu_1–O_3 = 104.9°. These values show that the set of O_2, O_3, N_1, N_2, and O_{14} atoms builds a square pyramid leaning toward cyclohexylamine ligands. Thus, although the Cu_1–O_{14} distance is rather long to be considered as typical of semicoordination, the copper surrounding is often taken as a proof of such semicoordination. Also, this perchlorate builds a hydrogen bond with N_2 since N_2–O_{13} = 2.95 Å. We found difficulties in refining atomic coordinates of the other perchlorate. A Fourier difference map calculated in the $O_{21}O_{23}O_{24}$ plane shows three areas of very broad electronic density around the chlorine position. Refinement of these three positions considered as oxygen ones led to very large isotropic temperature factors of 20, 24, and 19, respectively. The position of the fourth oxygen atom O_{22} was refined to a lower isotropic factor, equal to 13. This can be related to the occurrence of a weak hydrogen bond supported by a distance N_1–O_{22} equal to 2.99 Å. Different schemes of disorder were assumed for the perchlorate anion but no improvement in refinement was found. Also, some high thermal vibrations for the atoms which are not attached to the copper atoms were found. Indeed, such a strong thermal vibration was observed for the three carbon atoms of each ring opposite to the carbon atom attached to nitrogen. Attempts to plot electron densities vs. coordinates for the Fourier peaks of these carbon atoms show no splitting, which probably means no disorder. Presently, the results obtained at 294 K led to $R = 0.069$. Angles and distances given in this paper are considered accurate enough for the purpose of magnetic study, although some standard deviations appear high.

Magnetic Properties. The temperature dependences of the molar magnetic susceptibilities for two samples coming from two different preparations are shown in Figure 3. The magnetic behavior is characteristic of pairs of antiferromagnetically coupled Cu(II). Upon cooling of the samples from 312 to 10 K, the susceptibilities increase, reach a maximum at about 210 K, decrease, and finally increase again below 60 K. This low-temperature behavior is most likely due to traces of noncoupled Cu(II) as impurity in our samples. The magnetic data obtained with pairs of antiferromagnetically coupled ions are generally corrected for monomeric impurity by assuming on the one hand that the magnetic behavior of the impurity follows a Curie law and on the other hand that its molar weight is identical with that of the dimeric complex.[24] These two hypotheses led for our samples to two corrected curves which are not exactly superposable. These curves closely follow the equation giving the temperature dependence of the molar magnetic susceptibility for a Cu(II) dimer:

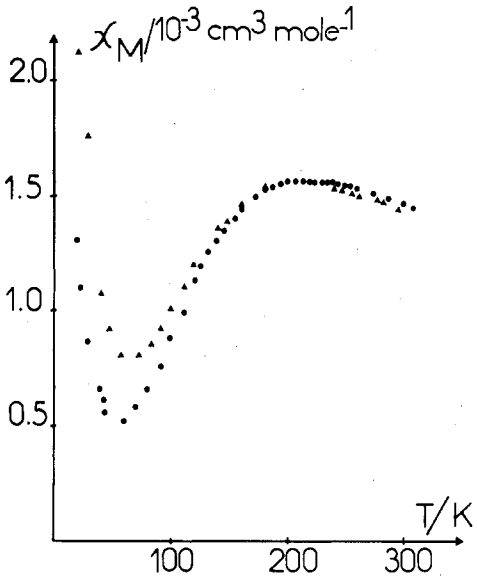

Figure 3. Experimental temperature dependence of the molar magnetic susceptibilities for samples A (●) and B (▲). The points ▲ between 180 and 230 K have not been indicated for clarity.

$$\chi_M = \frac{2N\beta^2g^2}{kT}\left[3 + \exp\left(-\frac{J}{kT}\right)\right]^{-1} + 2N\alpha \qquad (1)$$

where the symbols have their usual meaning, for two different values and too weak values of the g factor. Therefore, we took into account the fact that the ratio M_I/M_D of the molar weights for the impurity and the dimer might be different from unity (see Appendix I). For a ratio M_I/M_D equal to 1.60, the two corrected curves shown in Figure 4 become strictly identical and perfectly follow eq 1 for $g = 1.98$, $J = -256$ cm^{-1}, and $N\alpha$ negligible. The slightly too weak g value for the Cu(II) complex is not well understood. It could arise from the uncertainties on both ρ and M_D/M_I. On the other hand, the value of J does not depend on M_D/M_I and may be determined accurately. The uncertainty on J is estimated at ±2 cm^{-1} by comparing the effect of small changes in the parameters with the estimated experimental uncertainty. It is not useless to point out that the samples were prepared by carefully picking up small crystals under the microscope and that the chemical analyses were excellent (see Experimental Section); however, taking into account the low-temperature data and correcting the experimental curves for the very weak amount of monomeric impurity displace the maximum of χ_M about 15 K higher in temperature and significantly improve the determination of J. Without correction and only in the temperature range 77–300 K, did the fitting of the experimental data lead to a J value of −240 cm^{-1}.

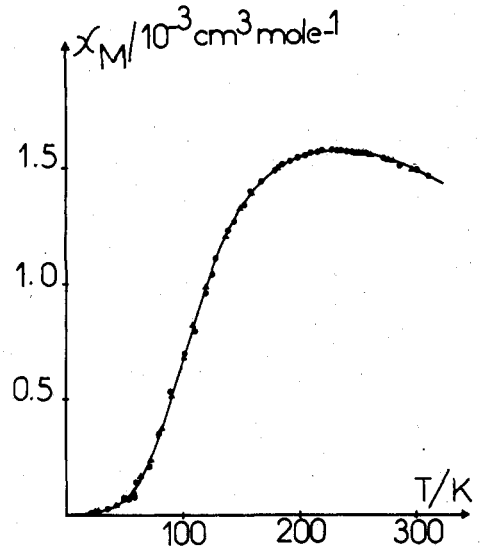

Figure 4. Magnetic data corrected from the noncoupled Cu(II) impurity for samples A (●) and B (▲) and theoretical curve (continuous line). For clarity the points ▲ between 180 and 230 K have not been indicated.

Owing to the structural differences, the comparison of the J value obtained for our compound with those reported for essentially planar hydroxo-bridged Cu(II) dimers may appear without heuristic interest. We wish to prove in the following discussion that such is not the case. For this discussion, we idealize somewhat the structure of the dimeric cation $[Cu(C_6H_{11}NH_2)_2OH]_2^{2+}$ by assuming the existence of a mirror plane containing the two hydroxo groups. This mirror plane does not exist in the crystal structure; however, the Cu_1–O_2 and Cu_2–O_2 distances are equal within standard deviations and the case is similar for Cu_1–O_3 and Cu_2–O_3 distances.

In an orbital model proposed by one of us,[25,26] the J singlet–triplet splitting in a Cu(II) dimer is expressed as the sum of an antiferromagnetic contribution J_{AF} and a ferromagnetic contribution J_F with

$$J_{AF} = -2\Delta S$$

$$J_F = 2\langle\phi_A(1)\phi_B(2)|r_{12}^{-1}|\phi_A(2)\phi_B(1)\rangle \qquad (2)$$

where ϕ_A and ϕ_B are the magnetic orbitals centered on A and B, respectively, S is the overlap integral $\langle\phi_A|\phi_B\rangle$, and Δ is the energy gap between the two molecular orbitals (MO) constructed from ϕ_A and ϕ_B. We showed that, at first order, S was proportional to Δ so that this gap Δ appears as the preponderant factor for J_{AF}.[27] From a different approach, Hoffmann was led to a similar result.[16]

In the planar hydroxo-bridged Cu(II) dimers, the increase of J when Cu–O–Cu decreases is explained as follows: the magnetic orbital for each Cu(II) ion is constructed from the d_{xy} metallic orbital (referring to the reference axes shown in Figure 5) pointing toward the bridging and terminal ligands. The interaction of the two magnetic orbitals leads to two MO's symmetric and antisymmetric, respectively, with regard to the mirror plane perpendicular to the Cu_2O_2 network. These MO's are antibonding with regard to the d metallic orbitals. The more important in absolute value the metal–ligand overlaps are, the more destablized the MO's. As shown by Hoffmann,[16] the variation vs. Cu–O–Cu of the metal–oxygen overlaps $S_x = |\langle d_{xy}|2p_x\rangle|$ and $S_y = |\langle d_{xy}|2p_y\rangle|$ exhibits a crossover for Cu–O–Cu = 90°. For Cu–O–Cu > 90°, we have $S_x > S_y$ and for Cu–O–Cu < 90°, the opposite situation holds. The variations vs. Cu–O–Cu of the energies ϵ_A and ϵ_S for the antisymmetric and the symmetric MO calculated from the FORTICON program[28] using the parametrization given in Appendix II are plotted in Figure 6. For the largest values

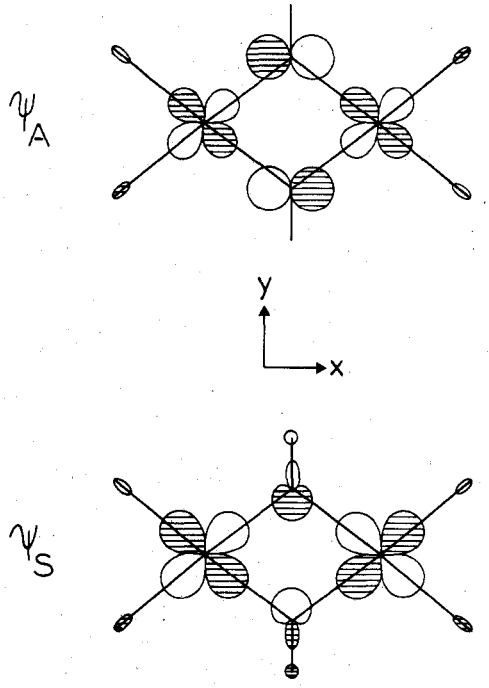

Figure 5. Schematic representation of the molecular orbitals built from the magnetic orbitals in hydroxo-bridged Cu(II) dimers.

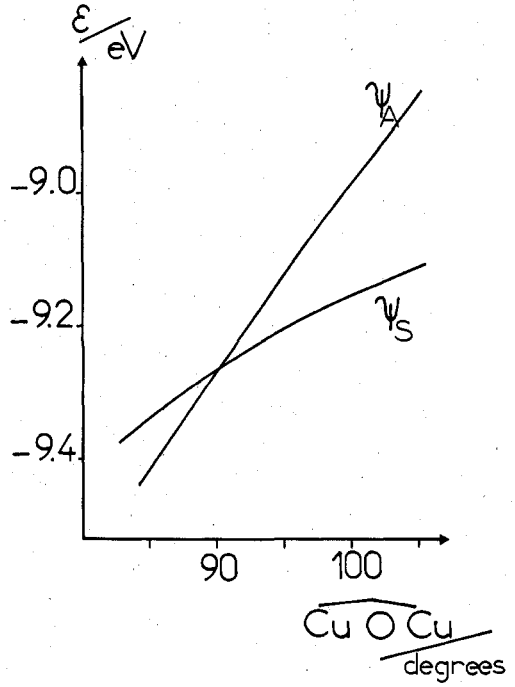

Figure 6. Variation vs. the bridging angle Cu–O–Cu of the energies of the symmetric ψ_S and antisymmetric ψ_A molecular orbitals for planar D_{2h} hydroxo-bridged Cu(II) dimers with Cu–O = 1.92 Å and Cu–O–Cu = 105.5°.

of Cu–O–Cu, $\Delta = \epsilon_A - \epsilon_S$ is large and J_{AF} is the preponderant contribution. J_{AF} diminishes in absolute value when Cu–O–Cu diminishes. For a peculiar value of Cu–O–Cu, experimentally observed at about 97.5°, J_{AF} and J_F exactly compensate themselves and for smaller values of Cu–O–Cu, J_{AF} becomes very weak and J_F is therefore the preponderant contribution. It must be noticed that in such an interpretation of the experimental data, it is implicitly assumed that J_F is constant whatever the Cu–O–Cu angle may be.

In order to compare our compound to the other hydroxo-bridged Cu(II) dimers, we propose to generate it in several

Scheme I

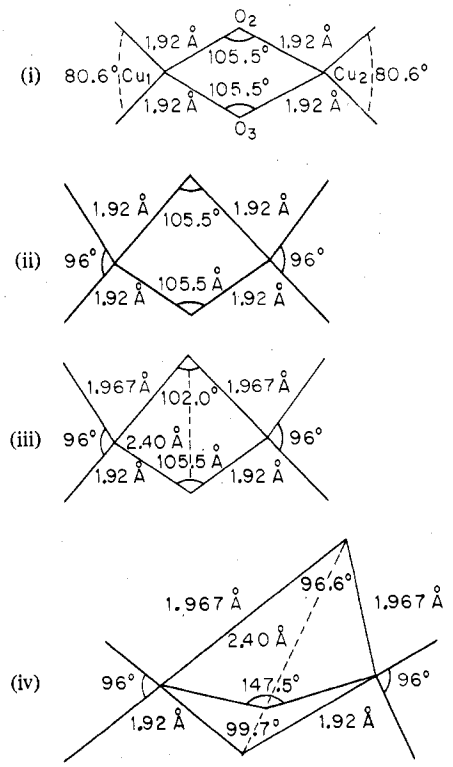

steps, according to Scheme I. (i) We start with a planar D_{2h} complex similar to those considered by Hatfield and Hodgson, the Cu–O distances being 1.92 Å and the Cu–O–Cu angles 105.5°. For such a complex, Hatfield and Hodgson's correlation (J/cm^{-1} = −74.53 Cu–O–Cu/deg + 7270) holds and leads to a J value close to −600 cm^{-1}. Our calculation of Δ gives 0.260 eV. (ii) The angles N–Cu–N are opened from 30°, which is their average value in the previously studied hydroxo-bridged Cu(II) dimers with bidentate terminal ligands, to the actual value in our complex of 96°. We checked that this opening of the N–Cu–N angles has no effect on the Δ value. (iii) An oxygen atom, say O_2, is displaced along a twofold axis so that we have a planar C_{2v} complex with $Cu_1–O_2 = Cu_2–O_2$ = 1.967 Å and $Cu_1–O_2–Cu_2$ = 102.0°. This lengthening of $Cu–O_2$ has a weak influence on Δ. As a matter of fact, when the $Cu–O_2$ distance increases, the overlap $S_x(Cu–O_2)$ decreases whereas the overlap $S_y(Cu–O_2)$ remains nearly constant. This favors a decrease of $\Delta = \epsilon_A - \epsilon_S$. This effect is compensated by the fact that the π-type oxygen–oxygen $\langle 2p_x|2p_x\rangle$ overlap remains negligible whereas the σ-type $\langle 2p_y|2p_y\rangle$ overlap in absolute value decreases. In the symmetric MO, the oxygen–oxygen interaction is antibonding; thus a decrease of $|\langle 2p_y|2p_y\rangle|$ favors an increase of Δ. For this structure, we get Δ = 0.268 eV. (iv) The reader has likely already noticed that the previous structure may be deduced from the actual structure of $[(C_6H_{11}NH_2)_2CuOH]_2^{2+}$ by opening the binuclear cation, in the same way as one opens a book, to obtain a planar Cu_2O_2 network. During this, the $O_2–O_3$ distance is retained but the $Cu_1–Cu_2$ distance and the two Cu–O–Cu angles are modified. Thus, the last step consists of bending the previous structure in order to obtain a C_s symmetry with a dihedral angle of 147.5°. In such a modification, the $S_x(Cu–O_2)$ and $S_x(Cu–O_3)$ overlaps strongly decrease whereas the $S_y(Cu–O_2)$ and $S_y(Cu–O_3)$ overlaps are unchanged. As far as the oxygen–oxygen interactions are concerned, they are not modified since the oxygen–oxygen distance is maintained constant. Therefore, when the dinuclear cation is bent, the ϵ_A energy decreases and the ϵ_S energy is essentially unchanged. This result is shown in Figure 7. A

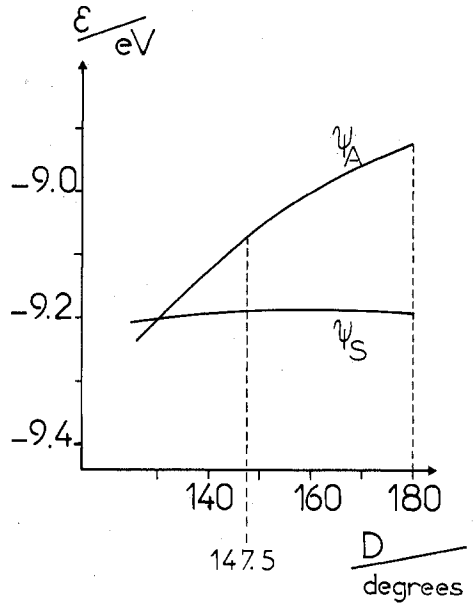

Figure 7. Variation vs. the dihedral angle D of the energies of the symmetric and antisymmetric molecular orbitals for roof-shaped hydroxo-bridged Cu(II) dimers with $Cu_1–O_3 = Cu_2–O_3$ = 1.92 Å, $Cu_1–O_2 = Cu_2–O_2$ = 1.967 Å, and $O_2–O_3$ = 2.40 Å.

Table V. Parameters Used in the Iterative Extended Hückel Calculation

atom	atomic orbital	A_μ	B_μ	C_μ	$g_{\mu\mu}$
Cu	4s	0.942	8.840	7.720	10.90
	4p	1.050	6.640	3.980	10.90
	3d	0.0	9.724	10.568	10.90
O	2s	0.0	15.20	33.00	15.20
	2p	0.0	15.20	16.40	15.20
N	2s	0.0	13.70	26.40	13.70
	2p	0.0	13.70	13.40	13.70
H	1s	13.618	27.180	13.60	12.80

crossover is found for a dihedral angle of 130°. In a general manner, when an hydroxo-bridged Cu(II) dimer is bent in such a way that the dihedral angle between the two $Cu–O_2$ planes diminishes, the oxygen–oxygen distance remaining constant, the energy gap between the symmetric and antisymmetric MO's diminishes and the coupling becomes less antiferromagnetic. This statement well corresponds to the J value found for the studied compound, −256 cm^{-1}, which is clearly stronger in algebraic value than it would be if the complex was planar. From here, it can be expected that with another roof-shaped hydroxo-bridged Cu(II) dimer with similar copper–oxygen and oxygen–oxygen distances, but with a smaller dihedral angle, the coupling would become more ferromagnetic. This might perhaps be obtained by changing the nature of the counteranions.

To conclude, we want to dwell on the fact that, even if the interpretation of the magnetic data proposed herein appears satisfying, it is incomplete. We again implicitly assume that the ferromagnetic contribution was roughly constant whatever the geometry modifications may be. Nothing theoretically justifies such an assumption. Moreover this ferromagnetic contribution may be important. So, in $[Cu(2,2'\text{-bpy})_2OH]_2(NO_3)_2$, J is equal to +172 cm^{-1};[29] this means that we have $J_F \geq 172$ cm^{-1}. In a Co(II)–Cu(II) heterobinuclear complex with orthogonal magnetic orbitals, a J_F value of several hundreds of wavenumbers has been reported.[30] Finally, as we have already done in previous papers, we want to emphasize the need of further and decisive progress in the understanding of the main factors governing the magnitude of the ferromagnetic coupling. We hope to be able in the

future to propose some new results in this matter.

Appendix I

Each sample contains a mass m_D of Cu(II) dimer and a mass m_I of monomeric Cu(II) impurity. Let us note M_D, χ_g^D and χ_M^D and M_I, χ_g^I and χ_M^I the molar weights, the susceptibilities per gram, and the molar susceptibilities for the dimer and the impurity, respectively. The apparent susceptibility per gram χ_g of the sample is given by

$$\chi_g = \chi_g^D \frac{m_D}{m_D + m_I} + \chi_g^I \frac{m_I}{m_D + m_I}$$

and the apparent molar susceptibility χ_M is

$$\chi_M = \chi_M^D \frac{m_D}{m_D + m_I} + \chi_M^I \frac{M_D}{M_I} \frac{m_I}{m_D + m_I}$$

$$\chi_M = \chi_M^D(1 - \rho M_I/M_D) + \chi_M^I \rho$$

where $\rho = [m_I/(m_D + m_I)](M_D/M_I)$ can be determined for each sample from the low-temperature data, by assuming that χ_M^I follows a Curie law: $\chi_M^I = N\beta^2 g^2/4kT$. The ratio M_I/M_D can be determined only from the study of several samples by using a self-consistent procedure.

Appendix II

The calculation performed in this work is of extended Hückel type, with charge iteration on all the atoms and Madelung corrections. The actual terminal ligands are replaced by ammonia molecules. The atomic orbitals are simple Slater-type orbitals for hydrogen, nitrogen, oxygen, and copper except for metallic 3d orbitals for which we choose two-component orbitals. Orbital exponents for the nonmetallic atoms are chosen by using Slater's rules; 4s and 4p exponents for copper come from Burns,[31] assuming a charge +1 on the transition ions in the complex. Exponents and relative weights for metallic 3d orbitals are taken from Richardson et al.[32] The A_μ, B_μ, C_μ, and $g_{\mu\mu}$ parameters of the method are given in Table V. The K parameter of the Wolfsberg–Helmholz approximation is taken equal to 1.75.

Registry No. $[Cu(C_6H_{11}NH_2)_2OH]_2(ClO_4)_2$, 35637-92-4.

Supplementary Material Available: A listing of structure factor amplitudes (24 pages). Ordering information is given on any current masthead page.

References and Notes

(1) (a) Laboratoire de Spectrochimie des Elêments de Transition, Equipe de Recherche Associée au CNRS No. 672, Orsay. (b) Laboratoire de Chimie des Métaux de Transition, Equipe de Recherche Associée au CNRS No. 608, Paris.
(2) D. M. Duggan and D. N. Hendrickson, *Inorg. Chem.*, **12**, 2422 (1973); **13**, 2929 (1974).
(3) G. R. Hall, D. M. Duggan, and D. N. Hendrickson, *Inorg. Chem.*, **14**, 1956 (1975).
(4) E. J. Laskowski, D. M. Duggan, and D. N. Hendrickson, *Inorg. Chem.*, **14**, 1205 (1975).
(5) E. Sinn, *Inorg. Chem.*, **15**, 366 (1976).
(6) V. H. Crawford, H. W. Richardson, J. R. Wasson, D. J. Hodgson, and W. E. Hatfield, *Inorg. Chem.*, **15**, 2107 (1976), and references therein.
(7) W. E. Hatfield, *ACS Symp. Ser.*, **No. 5**, 108 (1974), and references therein; D. J. Hodgson, *Prog. Inorg. Chem.*, **19**, 173 (1975).
(8) J. A. Bertrand, J. H. Smith, and D. G. Van Derveer, *Inorg. Chem.*, **16**, 1477, 1484 (1977).
(9) T. R. Felthouse, E. J. Laskowski, and D. N. Hendrickson, *Inorg. Chem.*, **16**, 1077 (1977).
(10) J. Moreland and R. J. Doedens, *Inorg. Chem.*, **17**, 674 (1978).
(11) T. R. Felthouse and D. N. Hendrickson, *Inorg. Chem.*, **17**, 444 (1978).
(12) R. B. Wilson, J. R. Wasson, W. E. Hatfield, and D. J. Hodgson, *Inorg. Chem.*, **17**, 641 (1978).
(13) E. J. Laskowski and D. N. Hendrickson, *Inorg. Chem.*, **17**, 457 (1978).
(14) E. F. Hasty, L. J. Wilson, and D. N. Hendrickson, *Inorg. Chem.*, **17**, 1834 (1978).
(15) J. J. Girerd, S. Jeannin, Y. Jeannin, and O. Kahn, *Inorg. Chem.*, **17**, 3034 (1978).
(16) P. J. Hay, J. C. Thibeault, and R. Hoffmann, *J. Am. Chem. Soc.*, **97**, 4884 (1975).
(17) A. T. Casey, B. F. Hoskins, and F. D. Whillans, *Chem. Commun.*, 904 (1970); *J. Chem. Soc., Dalton Trans.*, 1267 (1975).
(18) A. Bencini and D. Gatteschi, *Inorg. Chim. Acta*, **31**, 11 (1978).
(19) (a) J. Karle and H. Hauptman, *ACA Monogr.*, **No. 3**, (1953); (b) D. Rogers, E. R. Howells, and D. C. Phillips, *Acta Crystallogr.*, **3**, 210 (1960).
(20) D. T. Cromer and J. T. Waber, *Acta Crystallogr.*, **18**, 104 (1965).
(21) R. F. Stewart, E. R. Davidson, and W. T. Simpson, *J. Chem. Phys.*, **42**, 3175 (1965).
(22) C. K. Johnson, personal communication, 1965.
(23) B. N. Figgis and J. Lewis, *Mod. Coord. Chem.*, 403 (1960).
(24) A. P. Ginsberg, *Inorg. Chim. Acta Rev.*, **5**, 45 (1971).
(25) O. Kahn and B. Briat, *J. Chem. Soc., Faraday Trans. 2*, **72**, 268 (1976); *Colloq. Int. C.N.R.S.*, **No. 255**, 251 (1976)
(26) J. J. Girerd, M. F. Charlot, and O. Kahn, *Mol. Phys.*, **34**, 1063 (1977).
(27) O. Kahn, B. Briat, and J. Galy, *J. Chem. Soc., Dalton Trans.*, 1453 (1977).
(28) Forticon 8, No. 344, Quantum Chemistry Program Exchange, Indiana University, Chemistry Department.
(29) K. T. McGregor, N. T. Watkins, D. L. Lewis, R. F. Drake, D. J. Hodgson, and W. E. Hatfield, *Inorg. Nucl. Chem. Lett.*, **9**, 423 (1973).
(30) O. Kahn, R. Claude, and H. Coudanne, *J. Chem. Soc., Chem. Commun.*, 1012 (1978).
(31) G. Burns, *J. Chem. Phys.*, **41**, 1321 (1964).
(32) J. W. Richardson, W. C. Nieuwpoort, R. R. Powell, and W. F. Edgell, *J. Chem. Phys.*, **36**, 1057 (1962).

Contribution from the Institute of Physical and Chemical Research, Wako-shi, Saitama, 351 Japan

Neutral and Cationic Rhodium Complexes of 2,6-Disubstituted Phenyl Isocyanides. Crystal Structure Analysis of Chlorotris(2,4,6-tri-*tert*-butylphenyl isocyanide)rhodium(I) and Estimation of Bulkiness in Isocyanide Substituent[1]

YASUHIRO YAMAMOTO,* KATSUYUKI AOKI, and HIROSHI YAMAZAKI

Received November 27, 1978

Reaction of $[Rh(COD)Cl]_2$ with 2,6-xylyl isocyanide gave $Rh(C_9H_9N)_3Cl$ (**1a**) or $[Rh(C_9H_9N)_4]Cl$ (**2a**), depending on the molar ratio of the starting compounds, whereas reaction with 2,4,6-tri-*tert*-butylphenyl isocyanide gave only $Rh(C_{19}H_{29}N)_3Cl$ (**1g**). Treatment of **1g** with $C_{19}H_{29}N$ in the presence of $AgPF_6$ led to formation of cationic $[Rh(C_{19}H_{29}N)_4]PF_6$ (**2g**). Compound **2a** has a tendency to self-associate in solution, but no association occurred in **2g**, due to steric hindrance of bulky isocyanide ligands. Compound **1g** crystallizes in space group $P\bar{1}$ with two molecules in a unit cell of dimensions a = 14.750 (5) Å, b = 23.785 (7) Å, c = 10.193 (5) Å, α = 104.71 (2)°, β = 104.65 (2)°, and γ = 71.59 (1)°. Each phenyl ring of the isocyanide ligands lies in a plane perpendicular to the $RhClC_3$ plane. The steric bulkiness of isocyanides was estimated in terms of fan-shaped angles.

There has been recent interest in investigations of the ground- and excited-state physical and chemical properties of complexes in which metal(d^8)–metal(d^8) interactions are present.[2] It has been reported that the planar rhodium isocyanide cations, $Rh(RNC)_4^+$ (R = Ph, Et, CH_3, etc.), undergo self-association in solution presumably through direct met-

0020-1669/79/1318-1681$01.00/0